Experimental discrimination of geminate and non-geminate recombination in a-Si:H

T. W. Herring,[1] S.-Y. Lee,[1] D. R. McCamey,[1] P. C. Taylor,[2] K. Lips,[3] J. Hu,[4] F. Zhu,[4] A. Madan,[4] and C. Boehme[1,*]

[1]*Department of Physics and Astronomy, University of Utah, 115S 1400E, Salt Lake City, Utah 84112, USA*

[2]*Department of Physics, Colorado School of Mines, 1523 Illinois Street, Golden, Colorado 80401, USA*

[3]*Helmholtz-Zentrum Berlin für Materialien und Energie (formerly Hahn-Meitner-Institut), Institut Silizium-Photovoltaik, Kekulésstr 5, D-12489 Berlin, Germany*

[4]*MVSystems, Inc., 500 Corporate Circle, Suite L, Golden, Colorado 80401, USA*

(Received 7 August 2008; revised manuscript received 19 February 2009; published 12 May 2009)

A study of charge-carrier recombination in intrinsic hydrogenated amorphous silicon (a-Si:H) is presented using pulsed electrically and pulsed optically detected magnetic-resonance spectroscopies in order to measure the influence of spin-dependent recombination on photoluminescence (PL) and photoconductivity (PC). The experiments show band tail state recombination influencing the PL but not the PC which constitutes geminate recombination of correlated charge carriers that do not contribute to charge transport. In contrast, nongeminate recombination through silicon dangling bonds is observed influencing both PL and PC. The experiments presented constitute a direct and unambiguous observation of geminate and nongeminate recombination in a-Si:H.

DOI: 10.1103/PhysRevB.79.195205 PACS number(s): 76.70.Hb, 71.23.Cq, 73.50.Gr, 76.90.+d

I. INTRODUCTION

The nature of geminate recombination (recombination of an electron and hole created by the same photon) and nongeminate recombination in disordered solids has been debated for many years, but definitive results in any test material have been elusive.[1–7] This problem applies equally to inorganic and organic solids as diverse as amorphous silicon and disordered fullerenes and because it is critical for understanding the operation of important electronic devices, such as solar cells and light emitting diodes.

In the following, we describe the first definitive separation of geminate and nongeminate recombination using hydrogenated amorphous silicon (a-Si:H) as a prototypical test bed since a-Si:H is one of the most widely used materials for photovoltaic applications and other electronic devices ranging from thin-film transistors to radiation detectors.[1,8] The band structure, charge transport, and recombination mechanisms of a-Si:H have been investigated intensively and a qualitative picture, as illustrated in Fig. 1, has emerged.[1,2,8–14] A-Si:H is a disordered semiconductor whose band gap is filled with localized states. At energies close to the mobility edges, which separate localized from extended electronic states, high densities of band tail states exist which decline exponentially toward the band-gap center. Deep in the band gap, unsaturated silicon bonds [called dangling-bond (db) states] are found. As the correlation energies of defects in a-Si:H are generally positive, band-gap states can be paramagnetic, making electron-spin resonance (ESR) spectroscopy an extraordinarily successful method for their investigation.[3,11,12,15–18] ESR studies have shown that defects in a-Si:H have broadly distributed Landé factors around $g \approx 2.004$ for conduction-band tail states, $g \approx 2.0055$ for dbs, and $g \approx 2.012$ for valence-band tail states.[11,12,14,15,18,19] There are various recombination mechanisms in a-Si:H involving some or all of these band-gap states. Due to disorder, any recombination mechanism always represents a large group of quantitatively and even qualitatively different subgroups. Excitonic,[4,20,21] distant pair,[2,13,21] geminate, and nongeminate[2,5,6] processes have been discussed for a-Si:H in the past. Thus, recombination in a-Si:H is extraordinarily complex, and after decades of research, there still remain open questions about its fundamental properties and among those is the question of how to experimentally distinguish geminate from nongeminate recombination.

Geminate recombination does not influence photoconductivity (PC) even though it can cause photoluminescence (PL). In contrast, nongeminate recombination does influence PC strongly and it is therefore a determining factor for excess charge carrier lifetimes (see Fig. 1). Attempts to experi-

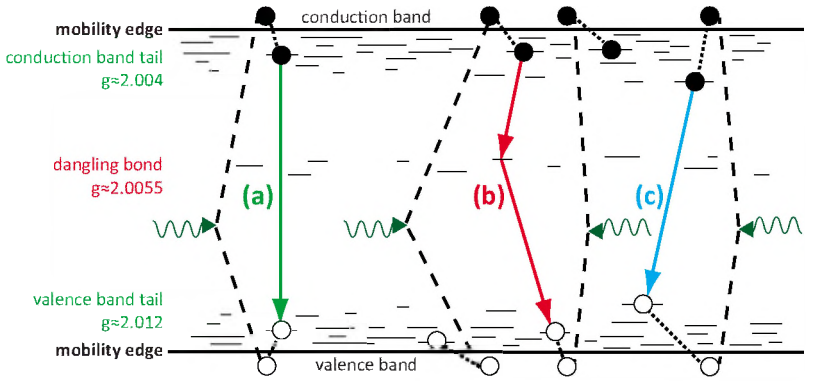

FIG. 1. (Color online) The band diagram of a-Si:H indicating the localization edges and the different types of localized band-gap states as well as the literature values for the Landé factors. The arrows indicate qualitatively different recombination channels discussed in text, namely, geminate band-tail state to band-tail state recombination between (a) strongly exchange and (c) weakly exchange-coupled pairs and (b) nongeminate recombination through dbs.

mentally discriminate geminate and nongeminate processes have been undertaken in the past.[1–6] One approach was suggested by Homewood *et al.*[3] who proposed to use electrically detected magnetic-resonance (EDMR) and optically detected magnetic-resonance (ODMR) spectroscopies, respectively, which are indirect ESR detection methods based on the magnetic-resonance-induced change in the spin of paramagnetic centers involved in spin-dependent recombination processes.[18] When a certain g factor is excited with microwave fields, the spin-dependent recombination rates of the corresponding spins will change. EDMR and ODMR highlight distinct recombination channels. As EDMR can only detect nongeminate recombination and ODMR is sensitive to both geminate and nongeminate recombinations, a comparison of both EDMR and ODMR allows us to discriminate geminate from nongeminate processes. While the approach of Homewood *et al.* is feasible in principle, experimental progress has been minimal as ODMR spectra of a-Si:H cannot easily be deconvoluted into distinguishable peaks since the broad ODMR lines merge into one feature.[14]

In the following we present an experimental study on nominally intrinsic a-Si:H that directly and unambiguously allows us to discriminate geminate from nongeminate recombination by using pulsed (p) coherent ODMR and EDMR instead of the traditional continuous-wave methods. As demonstrated recently,[14] pODMR cannot only resolve g factors associated with a recombination channel but also the qualitative and quantitative coupling between the recombining charge carriers through the observation of spin Rabi nutation which allows a two-dimensional mapping (g,Ω) of different recombination channels. Superpositions of different recombination mechanisms with similar g factors can be disentangled experimentally by using this measurement approach. As recombination detected with pODMR is then compared to recombination detected with pEDMR, signals which influence PL, but not PC, can be attributed to geminate recombination while signals influencing both PL and PC or PC only can be identified as nongeminate recombination.

II. EXPERIMENTAL METHODS

The experimental data were obtained from nominally intrinsic device grade a-Si:H. As identical measurement conditions are crucial for comparison of the pODMR with the pEDMR measurements, it was necessary that both experiments were conducted on identical materials under identical temperatures, illumination, magnetic, and microwave fields. For the pODMR experiments we used a 2 mm $\times$ 2 mm $\times$ 300 nm thick intrinsic a-Si:H film which was deposited by plasma enhanced chemical vapor deposition (PECVD) at MVSystems, Inc., where extensive studies on reliability and reproducibility of a-Si:H deposition have been conducted. A single excitation fiber was used to couple light onto the sample. The fiber was aligned to ensure homogeneous illumination and also to control the intensity, which was kept at $I=400(10)$ mW/cm^2. The excitation light was a green line ($\lambda=514$ nm) of an Ar^+ ion laser. The PL was detected over an integrated wavelength range of 1050 nm $\leq\lambda\leq$ 650 nm using a silicon detector via a fiber bundle and a long-wave-pass edge filter. The sample temperature was $T=15$ K where maximal relative PL changes could be observed with pODMR. For both the pODMR and the pEDMR experiments, we placed a phosphorous-doped crystalline silicon sample as a spin standard in close proximity (<1 mm) to the a-Si:H samples in order to calibrate absolutely the B_0 field as well as the microwave field B_1 whose strength was needed for the transient nutation measurements. The B_1 calibration was conducted by simultaneous ESR detected transient nutation of the phosphorous donor-electron spins.

A key challenge for the experiments was to conduct pEDMR at $T=15$ K. As hopping transport dominates at this temperature, the conductivity of a-Si:H is very low and metal contacts to intrinsic a-Si:H are poor due to barrier formation. To overcome this problem we follow the approach of Ref. 3 using a *p-i-n* structure with a thick ($\approx$300 nm) *i* layer and thin ($\approx$15 and $\approx$6 nm) *n* and *p* layers. The *p-i-n* layer is essentially a solar cell with excellent ohmic contacts at low temperatures which allows pEDMR measurements at a photovoltaic operation point where the absolute sample current is very sensitive to the changes in recombination. The *p-i-n* device stack was deposited on top of a transparent conducting ZnO layer in a multichamber PECVD/sputter cluster tool system, at a substrate temperature of 200 °C, a power density of $P=17$ mW/cm^2, and an excitation frequency of $f=13.56$ MHz. The EDMR device area was 2×2 mm^2 located at the tip of a 3 mm wide times 50 mm long substrate with two contact pads located at $\approx$45 mm distance from the device. This long thin-film contact geometry follows a design used before for pEDMR samples.[22] The illumination of the sample during the pEDMR experiment took place through a window in the resonator. To ensure comparability, we verified that internal fields of the *p-i-n* structures do not cause a relevant change in the spin-dependent processes within the device compared to pure a-Si:H samples. This was done by comparison of ODMR spectra from both the pure a-Si:H samples and pin structures which showed identical spectra.

III. EXPERIMENTAL RESULTS

Both the pEDMR and pODMR experiments were carried out in an identical transient nutation experiment[14,22] where, in the presence of an external constant magnetic-field B_0, a coherent microwave pulse drives an ESR-induced Rabi-nutation of paramagnetic centers involved in recombination for the duration of its pulse length τ (typically on a ns range). After the pulse, the changed electronic spin states cause changes in recombination rates whose gradual (microseconds range) relaxation to a steady state is recorded. Figure 2(a) displays the PL change ΔPL and the conductivity change ΔPC as functions of time t after a short microwave pulse of length $\tau=320$ ns that ends at $t=0$. For the two experiments, the magnetic field of $B_0\approx340$ mT and the microwave frequency $f\approx9.7$ GHz were tuned such that ESR was established for $g=2.008$ for the pODMR measurement and $g=2.0055$ for the pEDMR measurement. Both g factors correspond to the known signal maxima for ODMR and EDMR in a-Si:H, respectively. Note that both transients exhibit the

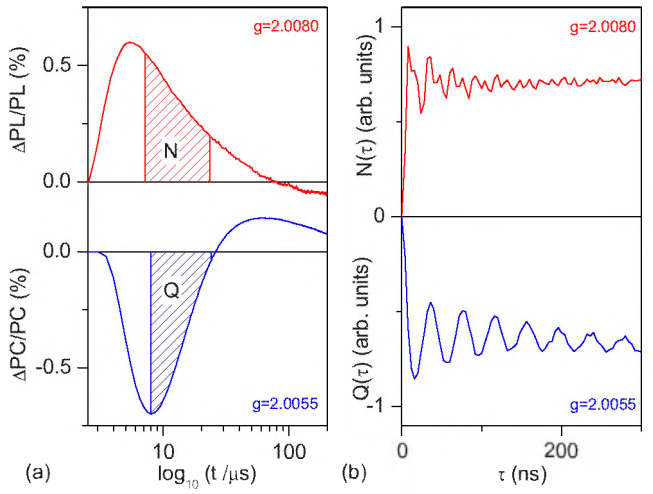

FIG. 2. (Color online) (a) Plot of the PL and the PC changes as functions of time after a short microwave pulse in ESR with $g=2.008$ and $g=2.0055$, respectively. (b) Plot of the photon number $N(\tau)$ and the charge $Q(\tau)$ as obtained by integration of the PL and PC, respectively [see shaded areas in (a)], as functions of the pulse length τ.

enhancement and quenching behavior as expected from previous[22] pEDMR and pODMR experiments. There is an initial recombination increase after the short ESR excitation followed by a temporary decrease due to the slowly recovering triplet population. While the enhancement or quenching behavior of recombination rates directly causes an enhancement or quenching behavior of the PL, it leads to a quenching or enhancement behavior of the PC as an increase in recombination decreases PC and vice versa. Both the PL and the PC measurements in Fig. 2(a) confirm previous transient pODMR (Ref. 14) and pEDMR (Ref. 22) measurements on a-Si:H.

The plots in Fig. 2(a) indicate time intervals over which we integrated ΔPL and ΔPC, yielding a photon number N and a charge Q (since PC $\propto$ current), respectively. N and Q are proportional to the singlet content of the spin state $|\Psi\rangle$ of the recombining charge carriers in ESR $[N,Q(\tau)\propto|\langle\Psi|S\rangle|^2]$.[22] Since $|\Psi(\tau)\rangle$ is a function of the pulse length τ, so are $N(\tau)$ and $Q(\tau)$, and thus, these functions represent the spin-Rabi nutation of the recombining charge carriers. Figure 2(b) shows $N(\tau)$ and $Q(\tau)$ for $\tau\leq 300$ ns. While both functions were recorded with identical B_1 fields, one can see a dramatic difference between the two nutation transients. The pODMR detected nutation shows various oscillation components indicating a variety of processes (confirming previous observations). In contrast, the pEDMR detected nutation resembles a modified Bessel function, as expected for pEDMR of a single recombination channel.[22]

We have repeated the measurements of $N(\tau)$ and $Q(\tau)$ for a range of $1.98\leq g\leq 2.04$. The fast Fourier transforms (FFT), FFT$[N(\tau)](g)$ and FFT$[Q(\tau)](g)$, of these measurements are displayed in Figs. 3(a) and 3(b). Note that the frequency scale Ω is normalized to the free electron-spin nutation frequency γB_1 where $\gamma\approx 28.024$ GHz/T is the gyromagnetic ratio.

IV. DISCUSSION

As expected from previous pODMR measurements of a-Si:H conducted at higher light intensities,[14] the data of Fig. 3(a) exhibit a number of distinct recombination channels which can be identified by means of their g factors and nutation frequencies. For $\Omega=\gamma B_1$, we see recombination of weakly coupled pairs with the strongest contributions at $g\approx 2.0055$. For $\Omega\approx\sqrt{2}\gamma B_1$, we see a broad symmetric structure almost throughout the measured g factor range that is centered around $g\approx 2.008$. The two maxima of this signal are close to the center which exhibits a minimum. As $g\approx 2.008$ is the average of the g factors of conduction ($g\approx 2.004$) and valence ($g\approx 2.012$) band tail states, this signal has been attributed to the convolution of Pake-type structured doublets due to the recombination of strong spin-dipolar coupled electrons and holes in band tail states. These states exhibit random distances and mutual orientations to the external magnetic field.[14] Finally, we observe a nutation signal with $\Omega=2\gamma B_1$ at $g\approx 2.008$, attributed to strong exchange-coupled pairs[23] of conduction-band and valence-band tail states in close proximity. These pairs may be referred to as excitons due to an exchange strength in excess of the Larmor frequency separation of the pairs; however, they do not resemble excitonic states discussed by Aoki *et al.*[4] which have exchange strengths in excess of the detectable X band pODMR limits. Figure 3(c) displays FFT$[N(\tau)]$ for four selected g factors collected with a higher number of averages compared to the data displayed in Fig. 3(a). These plots again confirm the presence of the three qualitatively different recombination channels discussed above.

Figures 3(b) and 3(d) show the data of pEDMR measurements of FFT$[Q(\tau)](g)$ for the same experimental conditions and parameter ranges as the pODMR data in Figs. 3(a) and 3(c). Here, one can see only a single contribution, namely, weakly coupled $\Omega=\gamma B_1$ pairs centered at $g\approx 2.0055$. In contrast, all the signatures due to conduction- and valence-band tails—band tail states observed with pODMR—are not strongly visible. Note that a weak influence of geminate recombination on the PC is possible due to second-order effects, such as extrinsic self-absorption. We have fit the B_0 field dependence of the FFT$[Q(\tau)]$ (not shown here) which revealed equally good agreements for a single db resonance, two band tail resonances, and even for combinations of both. Hence, the weakly coupled pairs observed may consist of both dbs, tail states or combinations of both, and in fact, these could be located in the i layer but also in the thin n layer as n-a-Si:H is known to cause an EDMR signal at $g=2.0045$.[24] In either case, the data unambiguously show that nongeminate spin-dependent recombination takes place through weakly coupled distant pair states. Hence, even though both the pODMR sample and the i layer of the pEDMR sample consist of identical intrinsic a-Si:H films, the measurements of recombination with pODMR and pEDMR under identical conditions show different and distinguishable spin-recombination mechanisms. Since there are several pODMR signals due to the i-a-Si:H layer but only one distinct contribution due to the entire p-i-n structure, there is no doubt that the recombination processes of strongly coupled charge carrier pairs observed with pODMR

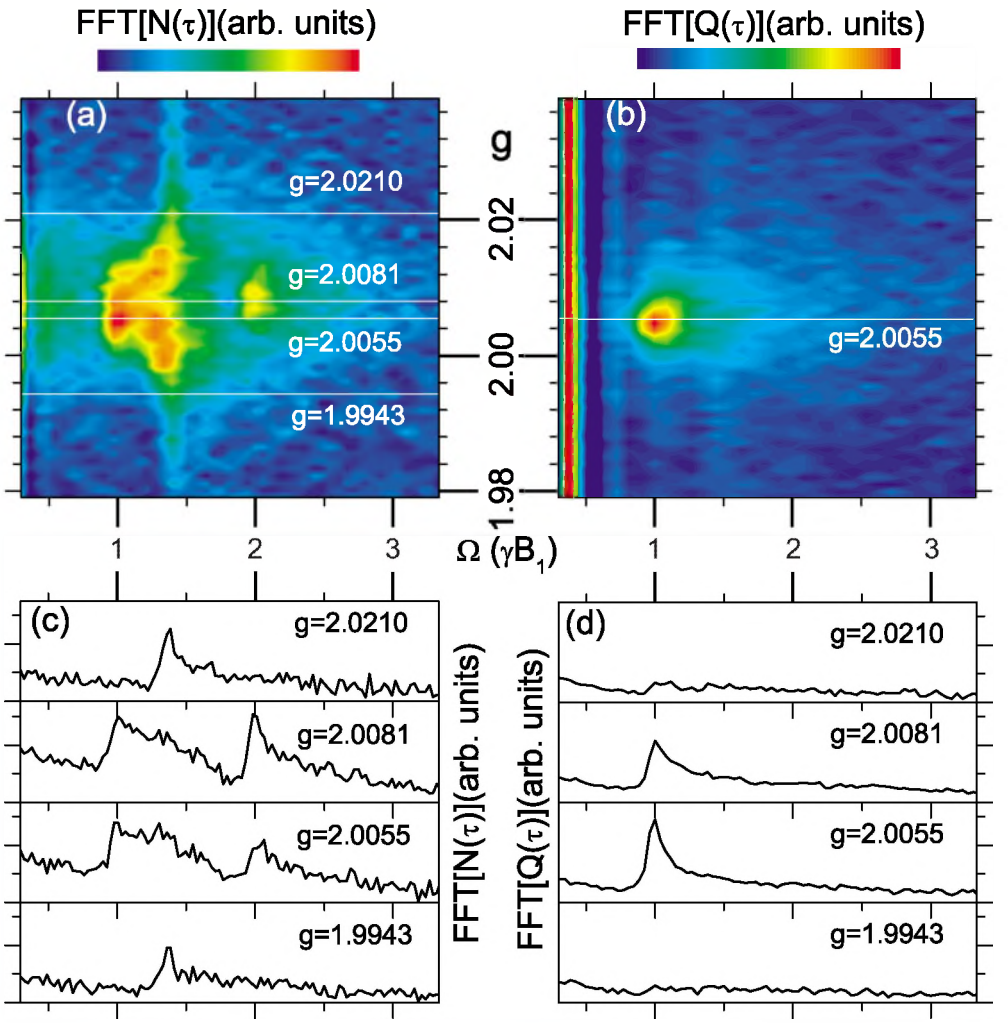

FIG. 3. (Color online) Three-dimensional plot of the FFT of the Rabi-nutation signals as a function of the g factor measured with (a) pODMR and (b) pEDMR under identical conditions. Plots for four selected g factors measured with (c) pODMR and (d) pEDMR under the same conditions as (a) and (b). The pODMR measurements reveal a number of recombination signals which are not detectable with pEDMR. Only one signal ($g=2.0055$, $\Omega=\gamma B_1$) is visible with with both pEDMR and pODMR.

are predominantly geminate. In contrast, the pEDMR data show strong contributions from weakly coupled spins only which are due to nongeminate recombination. We note that the data shown above represent recombination rate changes and not absolute rates, and we stress that these changes indicate spin-dependent transitions only. Thus, the larger number of pODMR signals compared to pEDMR does not indicate that geminate recombination is stronger than nongeminate recombination. The strength of the signals only prove the presence of the different mechanisms but not their dominance.

V. CONCLUSIONS

In conclusion, we find that a mapping of recombination in a-Si:H with pODMR and pEDMR confirms the presence of qualitatively distinct recombination processes, namely, recombination through (i) distant pairs of dbs and/or band tail states, (ii) strongly dipolar but weakly exchange-coupled band tail states, and (iii) strongly exchange-coupled band tail states. Only recombination through weakly coupled distant pairs influences PC significantly. Recombination through strongly coupled states is due to geminate processes only. We have demonstrated how to definitely discriminate geminate from nongeminate recombination in a-Si:H with an experimental procedure that is anticipated to allow further systematic investigations of recombination in a-Si:H and also in other disordered materials such as organic semiconductors.

ACKNOWLEDGMENTS

We gratefully acknowledge support from the DOE (through United Solar Ovonic) under Subcontract No. DE-FC36-07G017053, the NSF under Grant No. DMR0702351, and the BMBF (through the Helmholtz-Zentrum Berlin) under Grant No. EPR-Solar 03SF0328A. Acknowledgment is made to the donors of the American Chemical Society Petroleum Research Fund under Grant No. PRF 48916-DNI10 for partial support of this research.

*boehme@physics.utah.edu

[1] R. A. Street, *Hydrogenated Amorphous Silicon* (Cambridge University Press, Cambridge, England, 1991).
[2] P. Taylor, J. Non-Cryst. Solids **352**, 839 (2006).
[3] K. Homewood, B. Cavenett, W. Spear, and P. LeComber, J. Phys. C **16**, L427 (1983).
[4] T. Aoki, T. Shimizu, D. Saito, and K. Ikeda, J. Optoelectron. Adv. Mater. **7**, 137 (2005).
[5] R. Stachowitz, M. Bort, R. Carius, W. Fuhs, and S. Liedke, J. Non-Cryst. Solids **137-138**, 551 (1991).
[6] R. Stachowitz, M. Schubert, and W. Fuhs, Phys. Rev. B **52**, 10906 (1995).
[7] J. G. Muller, J. M. Lupton, J. Feldmann, U. Lemmer, M. C. Scharber, N. S. Sariciftci, C. J. Brabec, and U. Scherf, Phys. Rev. B **72**, 195208 (2005).
[8] *Hydrogenated Amorphous Silicon I and II*, edited by J. Joannopoulos and G. Lucovsky (Springer, New York, 2000).
[9] K. Morigaki, D. Dunstan, B. Cavenett, P. Dawson, and J. Nicholls, Solid State Commun. **26**, 981 (1978).
[10] R. A. Street, Phys. Rev. B **21**, 5775 (1980).
[11] H. Dersch, L. Schweitzer, and J. Stuke, Phys. Rev. B **28**, 4678 (1983).
[12] F. Boulitrop, Phys. Rev. B **28**, 6192 (1983).
[13] B. I. Shklovskii, H. Fritzsche, and S. D. Baranovskii, Phys. Rev. Lett. **62**, 2989 (1989).
[14] K. Lips, C. Boehme, and T. Ehara, J. Optoelectron. Adv. Mater. **7**, 13 (2004).
[15] M. Brodsky and R. Title, Phys. Rev. Lett. **23**, 581 (1969).
[16] P. A. Thomas, M. H. Brodsky, D. Kaplan, and D. Lepine, Phys. Rev. B **18**, 3059 (1978).
[17] K. Lips and W. Fuhs, J. Appl. Phys. **74**, 3993 (1993).
[18] M. Stutzmann, M. Brandt, and M. Bayerl, J. Non-Cryst. Solids **266-269**, 1 (2000).
[19] T. Umeda, S. Yamasaki, J. Isoya, and K. Tanaka, Phys. Rev. B **62**, 15702 (2000).
[20] B. A. Wilson, P. Hu, J. P. Harbison, and T. M. Jedju, Phys. Rev. Lett. **50**, 1490 (1983).
[21] H. Oheda, J. Appl. Phys. **101**, 053711 (2007).
[22] C. Boehme and K. Lips, in *Charge Transport in Disordered Solids with Applications in Electronics*, edited by S. Baranovski (Wiley, Chichester, 2006), Chap. 5, pp. 179–219.
[23] A. Gliesche, C. Michel, V. Rajevac, K. Lips, S. D. Baranovskii, F. Gebhard, and C. Boehme, Phys. Rev. B **77**, 245206 (2008).
[24] J. Behrends, A. Schnegg, C. Boehme, S. Haas, H. Stiebig, F. Finger, B. Rech, and K. Lips, J. Non-Cryst. Solids **354**, 2411 (2008).